Lung, Artificial: Basic Principles and Current Applications

William J. Federspiel
Kristie A. Henchir
University of Pittsburgh, Pittsburgh, Pennsylvania, U.S.A.

INTRODUCTION

Artificial lungs currently used or in development are medical devices designed to take over or supplement the respiratory function of the lung, which is to oxygenate the blood and remove carbon dioxide. Current artificial lungs are also known as blood oxygenators and are simple passive modules composed of bundles of hollow fiber membranes through which blood is pumped. Blood oxygenators are used routinely in cardiopulmonary bypass for open-heart surgical procedures. Much less prevalent is the use of artificial lungs in treating respiratory insufficiencies or failures, in applications generally known as Extracorporeal Membrane Oxygenation (ECMO) or Extracorporeal Life Support (ECLS). However, the growing incidence of lung disease associated with our aging population, along with advances in biomaterials, has spurred significant recent development work toward next-generation artificial lungs that could be used to successfully treat patients with a variety of respiratory failures.

Acute and chronic diseases of the lung remain major healthcare problems. Each year nearly 350,000 Americans die of some form of lung disease.[1] Overall, lung disease is America's number-three killer and is responsible for one in seven deaths. Adult respiratory distress syndrome (ARDS), only one form of acute lung failure, afflicts approximately 150,000 patients every year in the United States,[2] and despite advances in critical care medicine, ARDS mortality remains between 40% and 50%.[3,4] Most lung disease is chronic, and an estimated 30 million Americans are now living with chronic lung disease. Chronic obstructive pulmonary disease (COPD) includes emphysema and chronic bronchitis and afflicts over 16 million adults in the United States annually.[5] COPD is the fourth leading cause of death and the second most common disability. Each year nearly 400,000 COPD patients will be hospitalized with acute exacerbations of their chronic condition, a rate that has risen nearly threefold in the last decade.[6] Respiratory support for these patients is most often maintained using mechanical ventilation, and although adequate gas exchange may be achieved, ventilatory support can lead to barotrauma, volutrauma, and other iatrogenic injuries, further exacerbating the acute respiratory insufficiency in many patients.[7,8] Unlike mechanical ventilation, artificial lungs provide respiratory support independent of the lungs and allow a reversibly injured lung to rest and heal, thus offering the promise of improved treatment for acute respiratory insufficiencies or an effective bridge-to-lung transplant for chronic respiratory disease. Artificial lungs for longer-term respiratory support are likely far away, awaiting significant improvements in biomaterials and more efficient gas exchange strategies incorporated into their designs. Currently, lung transplantation remains the best treatment for chronic lung failures.

BACKGROUND

The natural lung represents a remarkable organ for gas exchange, and developing an artificial lung that approaches the gas exchange prowess of the natural lung is a significant engineering challenge. The alveoli of the lung, the tiny gas sacs at the termini of all the branching airways of the lung, offer intimate contact between inspired gas and blood flowing through capillaries in the lung (Fig. 1). The O_2 and CO_2 diffusing capacities of the lungs are proportional to the gas exchange area of the alveolar-capillary membrane and to the inverse of the diffusion distance across the alveolar-capillary membrane into blood.[9] The substantial gas exchange capacity of the lung stems from an alveolar-capillary area comparable to a tennis court surface, 100–150 m^2, packaged compactly with a high surface area to blood volume ratio of approximately 300 cm^{-1}[10] and a diffusion distance between gas and blood phases of no more than about 1–2 μm.[11] The natural lung can provide gas exchange ranging from resting levels for both O_2 and CO_2 (about 200–250 ml/min in average adults) to 10–20 times that under exercise conditions,[12] and it does so using room air as its oxygen supply gas. In contrast, current hollow fiber blood oxygenators, as used in cardiopulmonary bypass, have membrane areas ranging from 1 to 4 m^2 that are packaged much less compactly than in the natural lung, with a surface area to blood volume ratio 10 times less than in the natural lung (Fig. 2). The effective distance that gas diffuses between blood and gas flow pathways in artificial lungs is approximately 10–30 μm, an order

Encyclopedia of Biomaterials and Biomedical Engineering
DOI: 10.1081/E-EBBE 120007349

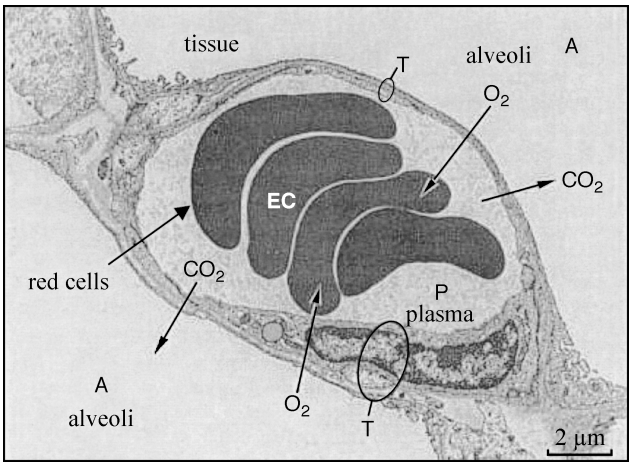

Fig. 1 The alveolar-capillary membrane in the natural lung showing intimate contact between inspired gas and blood in the lung. (Reprinted with written permission from Ref. 11, page 342, by Ewald R. Weibel/Harvard University Press.)

of magnitude greater than in the natural lung.[13] Thus, even with using 100% oxygen gas, artificial lungs currently used or under development aim at gas exchange levels that can support *resting* metabolic needs in patients. Artificial lungs that will allow patients any significant level of increased metabolic activity are not on the immediate horizon.

This article reviews artificial lung technology in terms of basic operational principles and present-day applications of standard blood oxygenators in cardiopulmonary bypass and ECMO/ECLS. Artificial lungs can be generally classified as extracorporeal, paracorporeal, intravascular, or intrathoracic (Fig. 3). The blood oxygenators used in cardiopulmonary bypass and ECMO/ECLS are

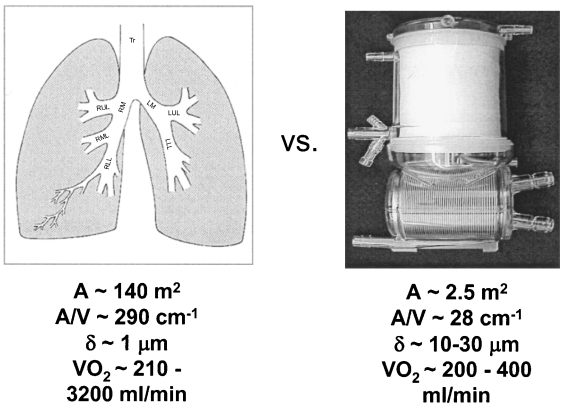

Fig. 2 Comparison of gas exchange parameters of the natural lung and current artificial lungs or blood oxygenators.

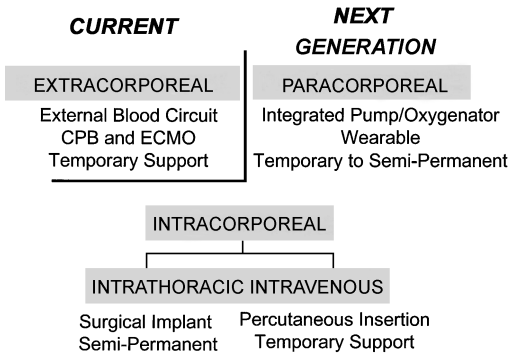

Fig. 3 Classification of artificial lung technology.

extracorporeal artificial lungs incorporated into pump-containing external blood circuits. The companion article to this one (see Lung, Artificial: Current Research and Future Directions) will review research and development work on next-generation paracorporeal, intravascular, and intrathoracic artificial lungs. This review will not cover the interesting and significant work on past artificial lungs, devices which are no longer in use or in development, such as bubble oxygenators, disc-type oxygenators, or even the early work based on hollow fiber membranes. For information pertaining to these earlier efforts in artificial lung development, the interested reader is referred to several previous comprehensive review articles.[13–15]

BASIC PRINCIPLES OF OPERATION

Hollow fiber membranes form the basic gas exchange units of contemporary artificial lungs and are small polymer tubes with microporous walls of 20 to 50 μm thickness and with outer diameters from 200 to 400 μm (Fig. 4). The wall pores have characteristic sizes typically below about 0.1 μm, and the porosity or volume fraction of the fiber wall can vary from about 30% to 50%.[16] Hollow fiber membranes for artificial lungs are made from hydrophobic polymers (often polypropylene), so that the membrane wall pores remain gas-filled and respiratory gases can diffuse readily across it. In most artificial lung applications, an oxygen (O_2) ''sweep gas'' flows through the inside lumens of the hollow fibers, while blood flows outside the hollow fibers through the interstitial spaces in the hollow fiber bundle. Oxygen diffuses down its concentration gradient across the fiber wall into blood, while carbon dioxide (CO_2) diffuses down its concentration gradient from the blood into the sweep gas flowing through the fibers and is removed when the sweep gas exits the device.

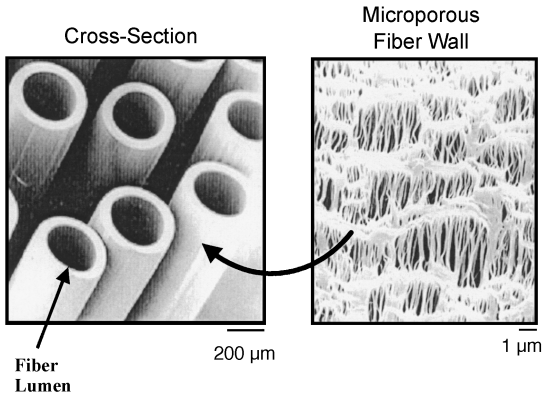

Fig. 4 Scanning electron micrograph of microporous hollow fiber membranes used in artificial lungs. The walls of the fibers (right) contain submicron pores where respiratory gases diffuse.

Determinants of Gas Exchange

The gas exchange permeance, K, of an artificial lung represents an overall mass transfer coefficient for either O_2 or CO_2 exchange.[9] The overall O_2 exchange rate, V_{O_2}, is related to the O_2 permeance according to

$$\dot{V}_{O_2} = K_{O_2} A(P_{O_{2g}} - P_{O_{2b}}) \quad (1)$$

where $P_{O_{2g}}$ and $P_{O_{2b}}$ are the *average* O_2 partial pressures in the sweep gas and blood phases, respectively, flowing through the artificial lung, and A is the total membrane area of the hollow fiber bundle. The gas exchange permeance for CO_2 removal can be related to the CO_2 exchange rate similarly using

$$\dot{V}_{CO_2} = K_{CO_2} A(P_{CO_{2b}} - P_{CO_{2g}}) \quad (2)$$

with the driving force for CO_2 exchange being the P_{CO_2} difference between blood and sweep gas. In artificial lungs the overall permeances for O_2 and CO_2 gas exchange are dictated by the diffusional resistances encountered as these gases diffuse between the sweep gas and blood flow pathways. Permeance is the inverse of a diffusional resistance, and the overall transfer resistance in an artificial lung device has two principal components:

$$\frac{1}{K} = \frac{1}{K_m} + \frac{1}{K_b} \quad (3)$$

where K_m and K_b are the membrane and blood-side permeances for each gas (O_2 and CO_2). The term $1/K_m$ represents a diffusional resistance for the membrane itself, while $1/K_b$ represents a resistance for gas diffusing between the membrane and the flowing blood stream.

Figure 5 illustrates the membrane and blood-side diffusional resistances to gas exchange in artificial lungs by showing the general gradient in CO_2 partial pressure from the sweep gas to the blood pathway. Transfer resistance within the sweep gas pathway is negligible. Most of the diffusional resistance resides within a blood-side diffusional boundary layer, and secondarily within the membrane itself. The blood-side and membrane permeances dictate overall gas exchange in artificial lungs and represent serial transport processes whose resistances add directly to determine overall resistance, as in Eq. 3. As serial ''resistors'' the smallest permeance or largest resistance controls overall gas exchange in an artificial lung.

Membrane Permeance

Most artificial lungs, including standard blood oxygenators, use microporous hollow fiber membranes. Microporous hollow fibers have fixed submicron pores within the wall that are contiguous from outer to inner lumen, and gas exchange occurs by diffusion through these gas-filled pores. The polymer used does not dictate gas exchange through the membrane as much as the pore characteristics and the fiber wall porosity. In artificial lungs the hydrophobic nature of the polymers (e.g., polypropylene) used to make the fiber membranes prevents intrusion of blood plasma into the fiber pores under normal conditions. Most microporous hollow fiber membranes for artificial lungs are manufactured by Celgard (Charlotte, NC), Membrana (Germany), and Mitsubishi Rayon (Japan). Table 1 summarizes the properties of several commercially available microporous hollow fibers commonly used in artificial lung devices.

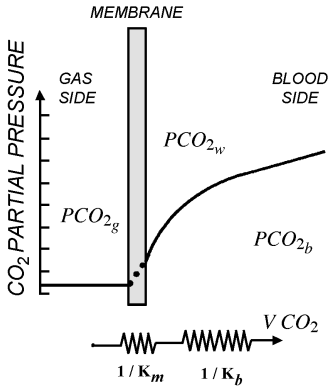

Fig. 5 Illustration of principal determinants of gas exchange in artificial lungs. PCO_{2w} represents the partial pressure of CO_2 at the membrane wall.

Table 1 Properties of commercially available hollow fiber membranes

Fiber	OD/ID (microns)	Wall thickness (microns)	Pore size (width × length) (microns)	Porosity
Celgard x30–240	300/244	28	0.03×0.2	40%
Mitsubishi KPF-190	245/200	22	0.04 (width)	40–55%
Membrana PP 50/280	380/280	50	0.2	N/A
DIC	255/205	25	Nonporous coated	Nonporous coated

The membrane diffusional resistance of a microporous hollow fiber depends on the permeance, K_m, of the fiber membrane. Membrane permeance is not usually reported by fiber manufacturers because its effect on the overall gas exchange performance of artificial lungs is negligible compared to blood-side permeance. The K_m for microporous hollow fiber membranes can be estimated theoretically using simple diffusion principles, and doing so predicts membrane permeances of approximately 2×10^{-2} ml/cm^2/s/cm Hg for O_2 and CO_2 gases in the Celgard X30-240 hollow fiber membrane.[17] The K_m of microporous hollow fibers can be measured using gas–gas test systems (i.e., with the fibers immersed in a gas rather than a liquid), so that all the transfer resistance is associated with the membrane. Kamo et al.[18] measured the oxygen permeance of the Mitsubishi KPF fiber as $K_m = 6.7 \times 10^{-2}$ ml/cm^2/s/cm Hg. Lund[16] determined K_m values of 1.72×10^{-2} and 1.47×10^{-2} ml/cm^2/s/cm Hg for O_2 and CO_2, respectively, at room temperature for the Celgard X30-240 fiber. A membrane permeance of 10^{-2} ml/cm^2/s/cm Hg for microporous hollow fibers represents a very large gas exchange capacity. For example, if membrane permeance dictated overall gas exchange, an artificial lung with 2 m^2 membrane area perfused with blood at a PCO_2 of 50 mm Hg would remove CO_2 at a theoretical rate of 60 liters per minute! The gas exchange rate of artificial lungs is much smaller than this because overall gas exchange is dictated by diffusional boundary layers that arise on fiber surfaces in the flowing blood stream. In practice, therefore, $K \cong K_b$ unless hollow fibers are coated with nonporous polymers (true membranes) to resist plasma wetting, as will now be described.

Membrane permeance can play an important role when coated or composite hollow fiber membranes are used to prevent plasma wetting in artificial lungs, a process in which blood plasma infiltrates the microporous walls of hollow fibers. Plasma wetting is a common problem when extracorporeal oxygenators are used in extended respiratory support and can lead to device failure within days.[19,20] Plasma wetting results primarily from phospholipids, lipoproteins and/or proteins in blood[19] that adsorb onto the fiber polymer surfaces at the plasma interface, rendering the interface hydrophilic and allowing for wetting of the pores by either partial or complete plasma infiltration. Plasma infiltration markedly diminishes the membrane permeance, K_m, because relatively rapid gas phase diffusion is replaced by diffusion through stagnant plasma within fiber pores. The membrane permeance for a completely wetted hollow fiber is in the range of 10^{-7} ml/cm^2/s/cm Hg for O_2, a 100,000-fold decrease compared with K_m for gas-filled pores.[17] Thus even partial plasma infiltration into fiber membranes can significantly reduce membrane permeance and degrade artificial lung performance.

Composite hollow fibers incorporate a thin nonporous polymer layer as a true membrane or ''skin'' on the microporous fiber surface (Fig. 6). The true membrane blocks infiltration of plasma into pores and is a key functional requirement of artificial lungs for longer-term

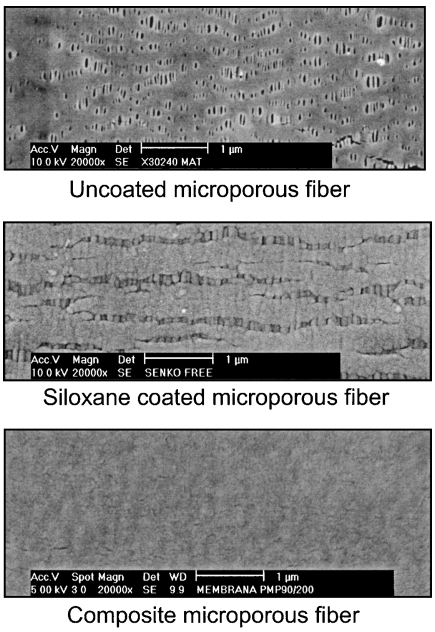

Fig. 6 SEMs of uncoated and coated hollow fiber membrane surfaces.

respiratory support. Composite hollow fiber membranes[18,21,22] are made either by coating an existing microporous fiber with a thin nonporous polymer (a true composite hollow fiber) or by modifying the fabrication of the microporous fiber itself to seal off pores at the surface (an asymmetric hollow fiber). The nonporous polymer skin that prevents plasma wetting also diminishes membrane permeance because a nonporous polymer can present an impediment to gas diffusion. Indeed, the membrane permeance of a composite hollow fiber is essentially dominated by the nonporous polymer layer and is given by

$$K_m = \frac{\alpha_P D_P}{\delta} = \frac{P_m}{\delta} \tag{4}$$

where α_p and D_p are the solubility and diffusivity of the gas within the nonporous polymer and δ is the polymer layer thickness. Polymer manufacturers usually report the *product* of polymer solubility and diffusivity, the polymer permeability (P_m) to specific gases. The design of composite hollow fiber membranes for artificial lungs requires a K_m that does not significantly reduce overall gas exchange. As an example, if coated or composite fibers are to exert no more than a 5% reduction in overall gas exchange for a particular artificial lung design, then K_m needs to be greater than 20 times K_b. For this reason, composite hollow fiber membranes for artificial lungs require nonporous polymers with relatively high gas permeabilities ($\sim$100 Barriers or greater[a]) that can be coated in a continuous layer of 1 μm thickness or less on microporous hollow fiber surfaces.[21]

Diffusional Boundary Layers

The blood-side permeance of an artificial lung, K_b, accounts for gas movement through the diffusional boundary layers that exist adjacent to the fiber surfaces, where fluid velocity is reduced by drag forces. Gas molecules traverse the boundary layer by molecular diffusion before being exposed to sufficient convection by the blood flowing past fiber surfaces. The blood-side permeance can be expressed as

$$K_b = \frac{\alpha_b D_b}{\delta_{bl}} \tag{5}$$

where α_b and D_b are the effective solubility and diffusion coefficient of the diffusing gas in blood and δ_{bl} is an average boundary layer thickness. For O_2 and CO_2 the effective solubility accounts for increased solubility due to hemoglobin binding (for O_2) or carriage as bicarbonate ion (for CO_2).

The boundary layer thickness, δ_{bl}, depends on the local interaction between diffusional and velocity fields in the flowing blood phase subjacent to the fiber surfaces of the artificial lung. The nature of these diffusional boundary layers is complex, but the simple boundary layer paradigm of laminar flow past a flat membrane surface can be instructive (Fig. 7). Boundary layer thickness on a flat surface grows with distance along the surface in the direction of flow according to

$$\delta_{bl}(x) \approx \left(\frac{v}{D_b}\right)^{1/6} \sqrt{\frac{D_b}{V} x} \tag{6}$$

where v is the kinematic viscosity, D_b is the species diffusion coefficient, and V is the bulk flow velocity past the surface.[23] An important concept is that boundary layer thickness can be decreased by increasing the blood flow velocity past the fiber surfaces, and the resulting increase in gas exchange permeance (see Eqs. 5 and 6) varies as the square root of flow velocity. Furthermore, because boundary layers grow along the fiber surface, permeance and gas exchange are less with *longitudinal* flow, parallel to the fiber axes, than with *transverse* or *cross* flow, perpendicular to the fiber axes. The simple boundary layer paradigm predicts that K_b for transverse versus longitudinal flow would be $K_b^{tran}/K_b^{long} \approx \sqrt{L/d}$, where L and d are fiber length and diameter, respectively. Since L/d in hollow fiber bundles can vary from 100 to 1000, an appreciable mass transfer benefit exists for transverse compared to parallel blood flow through hollow fiber bundles.

Mass Transfer Correlations

The blood-side permeability, K_b, for artificial lungs can be estimated from mass transfer correlations obtained for

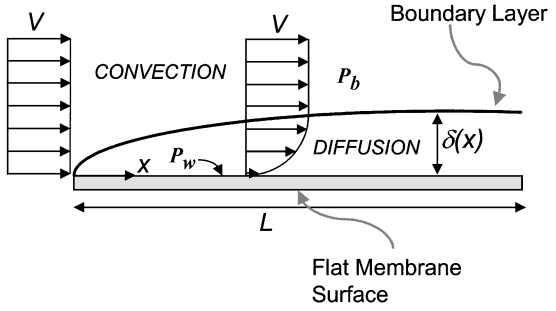

Fig. 7 Classical diffusional boundary layer on a flat surface. P_w represents the species partial pressure at the membrane wall.

[a]A Barrier is a common unit of polymer permeability and is equal to 10^{-10} ml-cm/cm^2/s/cm Hg.

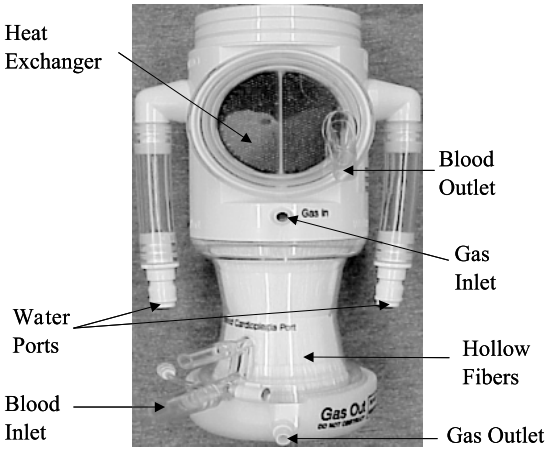

Fig. 8 A modern artificial lung showing the various ports for blood and gas flows. The heat exchanger warms the blood using water at 37°C.

flow through bundles of hollow fiber membranes. Convective mass transfer correlations have the general form[24]

$$Sh = aRe^{b}Sc^{1/3} \tag{7}$$

where Sh is the Sherwood number, $Sh = K_b d_h/\alpha D$; Re is the Reynolds number, $Re = Vd_h/v$; and Sc is the Schmidt number, $Sc = v/D$. These correlations involve the hydraulic diameter, d_h, of the fiber bed; the average interstitial blood flow velocity, V; the kinematic viscosity of blood, v; and the solubility, α, and diffusivity of the diffusing species in blood, D. Several studies[25–29] have reported mass transfer correlations in water and blood for steady flow through various module geometries of packed hollow fiber membranes, over a range of bundle porosities and Reynolds numbers. The a and b parameters in these mass transfer correlations depend on the fabricated fiber module, its porosity, and the flow patterns through the bundle. For example, Yang and Cussler[29] reported the correlation $Sh = 1.38Re^{0.34}Sc^{0.33}$ for flow through a 750-fiber bundle with a porosity of $\varepsilon = 0.3$, and the correlation $Sh = 1.9Re^{0.4}Sc^{0.33}$ for cross flow through a 72-fiber bundle with a much greater porosity of $\varepsilon = 0.93$. In the design of an implantable artificial lung, Vaslef et al.[30] used a correlation of $Sh = 0.52Re^{0.29}Sc^{0.33}$ based on measurements in a Sarns Membrane Oxygenator. Hewitt and Federspiel[24] averaged appropriate cross-flow correlations from the literature and used $Sh = 0.524Re^{0.523}Sc^{0.33}$ for model studies of gas exchange in an intravascular artificial lung. More complex correlations[31] were proposed for blood flowing through modules of cross-laid fiber mats oriented at various angles to the direction of blood flow.

Vaslef et al.[27] validated a useful method for using Sh versus Re correlations to relate O_2 exchange for water flow through an oxygenator bundle to that which would arise for blood flow through the same bundle. A dimensionless mass transfer correlation, $Sh = aRe^{b}Sc^{1/3}$, determined for a fiber bundle applies to blood and water alike (with same a and b constants), but the diffusivity in Sc number must appropriately account for hemoglobin binding of O_2 in blood. The Schmidt number involves an effective diffusivity dependent on the slope of the oxyhemoglobin dissociation curve:[24]

$$D_b^{eff} = \frac{D_b}{1 + C_{Hb}\dfrac{dS}{dP_{O_2}}\alpha_b^{-1}} \tag{8}$$

where C_{Hb} is hemoglobin concentration and S is hemoglobin saturation, while the Sherwood number involves the ordinary diffusivity of oxygen in blood, D_b. The permeance in blood depends on the blood P_{O_2} within the fiber bundle and can be 2–3 times that in water near the steep portion of the oxyhemoglobin dissociation curve.[24] The prediction of O_2 exchange in blood from water measurements worked well for several standard blood oxygenators,[27] and while a similar approach could be developed for relating CO_2 exchange in blood and water, none has yet to be specifically proposed or validated.

THE BLOOD OXYGENATOR

Artificial lungs that are used currently are membrane blood oxygenators consisting of either microporous polypropylene hollow fiber membranes or, as in one design, silicone sheets. The general anatomy of the oxygenator is similar between the two types of devices despite the differing gas exchange surfaces. Blood enters the oxygenator through an inlet port and flows either along the outside of the hollow fibers or the outside of the silicone sheet. The blood is then collected in a manifolded region, flows through a heat exchanger, and then exits the device through an outlet port. The gas, which can be pure oxygen or a mixture of oxygen and room air, enters the oxygenator through a gas inlet port, flows through the inside of the hollow fibers/silicone sheets, and exits the device via an outlet port (Fig. 8). The key design considerations in blood oxygenators include minimizing the resistance to blood flow, reducing the priming volume, ensuring easy debubbling at setup, and minimizing blood activation and thrombogenicity.

Most current blood oxygenators (Fig. 9) have fiber membranes with outer diameters of 200–400 μm and wall thickness of 20–50 μm, total membrane surface area of 2–4 m^2, and blood priming volume of 135–340 ml.[17] The hollow fibers are wound or matted within a hard plastic outer shell to produce fiber packing densities in the bundle

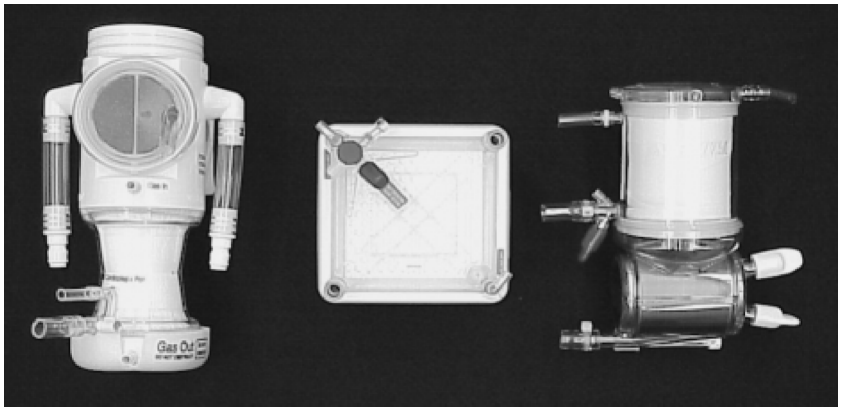

Fig. 9 Picture of currently used oxygenators. From left to right: Capiox® SX from Terumo Cardiovascular Systems, Quadrox® from Jostra, and Affinity® from Medtronic.

of 40–60%, and the arrangement of the fiber bundle and blood flow patterns differ between devices.[32] For example, fibers are helically wound in the Medtronic Affinity NT oxygenator. Blood enters the device through a central core channel and is then distributed radially through the fiber bundle. Fibers in the Jostra Quadrox oxygenator are aligned so that blood flow is perpendicular to the gas pathways. Hollow fiber oxygenators with intraluminal blood flow have been designed but are rarely used due to a generally unfavorable high resistance to blood flow.

The fabrication or wrapping of the fiber bundle in a blood oxygenator can be important as the geometry obtained impacts diffusional boundary layers, secondary flows, and gas exchange efficiency.[33] A blood oxygenator is often characterized by its rated flow as a measure of the gas exchange capacity of the device. Rated flow (see Fig. 10) is the flow rate through the oxygenator at which an inlet blood saturation of 70% can be oxygenated to an outlet blood saturation of 95%.[33] The rated flow can range from 1–1.8 l/min for a neonatal oxygenator and up to 7 l/min for an adult oxygenator (Table 2). A greater rated flow indicates an oxygenator with increased gas exchange capacity.

Silicone membrane oxygenators are often used in extracorporeal membrane oxygenation for respiratory support since plasma leakage does not occur as it does in microporous hollow fiber oxygenators. Kolobow[33] is generally credited with developing the first spiral-wound silicone membrane oxygenators in 1963. The oxygenator contains two silicone sheets sealed around the edges, which are wound around a polycarbonate core. Gas flows within the sealed sheets and blood flows countercurrently between the spiral wraps. The surface area of silicone membrane oxygenators ranges from 0.4 to 4.5 m^2 and the priming volumes range from 90 to 665 ml.[33] Because diffusion occurs across a nonporous silicone sheet, the

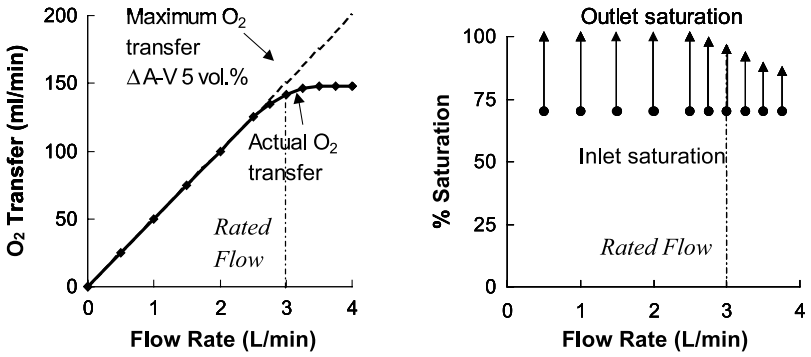

Fig. 10 The rated flow of a device is the maximum flow rate at which blood leaves the oxygenator at least 95% saturated. The rated flow depicted here is 3 l/min. (Adapted from Ref. [44].)

Table 2 Properties of blood oxygenators currently used clinically

	Membrane material[a]	Surface area (m^2)	Priming volume (ml)	Blood flow rate (l/min)	Rated blood flow (l/min)	Oxygen transfer (ml/min)
Terumo: Capiox SX10	P HFM	1	135	0.5–4.0	–	240
Terumo: Capiox SX18	P HFM	1.8	270	0.5–7.0	–	260
Terumo: Capiox SX25	P HFM	2.5	340	0.5–7.0	–	300
Jostra: Quadrox	P HFM	1.8	250	0.5–7.0	–	288
Avecor 0800	SMS	0.8	100	<1.2	1.2	70
Avecor 1500	SMS	1.5	175	1.0–1.8	1.8	113
Affinity	P HFM	2.5	270	1.0–7.0	7.0	374

[a]P, polypropylene; HFM, hollow fiber membranes; SMS, silicone membrane sheets.

thickness of these sheets was reduced to 100–200 μm. Nevertheless, the gas exchange efficiency of silicone oxygenators is substantially below that of hollow fiber oxygenators. The Avecor 0800 silicone oxygenator (a descendant of the Kolobow silicone oxygenator) has an O_2 transfer efficiency of 88 ml/min/m^2 compared to 150 ml/min/m^2 for the Affinity hollow fiber device.[33] The resistance to blood flow is also higher in silicone sheet oxygenators compared with hollow fiber oxygenators, and debubbling the sheet oxygenators can be more difficult.

Oxygenators in Cardiopulmonary Bypass

Cardiopulmonary bypass (CPB) using an external flow circuit incorporating a blood oxygenator is used in open-heart procedures to take over the function of both the heart and the lungs. Over 700,000 open-heart surgeries, including valve replacements, coronary artery bypass grafting, and heart transplants, were performed in the United States in 1999.[34] In cardiopulmonary bypass, blood is drained by gravity from the inferior/superior vena cava or the right atrium into a venous reservoir and is then pumped through the oxygenator by either a roller or centrifugal pump back into the ascending aorta (Fig. 11). Blood flow during CBP is kept low (2–2.4 l/m^2/min) to minimize bleeding.[35] A heat exchanger is required to cool and rewarm the patient and is typically incorporated into the oxygenator. Oxygen, or a mixture of oxygen and carbon dioxide, is fed through flowmeters and blenders into the oxygenator at flow rates of 5–10 l/min, which is 2–3 times the flow rate of blood.[36] The oxygenator must be capable of transferring up to 250 ml/min of oxygen and 200 ml/min of carbon dioxide during cardiopulmonary bypass in order to meet the metabolic needs of the patient.[36] The bypass circuit also includes suction devices that are used to maintain a blood-free surgical field. The suctioned blood is collected and filtered in a cardiotomy reservoir and is then pumped into the venous reservoir. Other components of the bypass circuit include pressure and temperature monitors, sampling ports, filters, tubing, and cannulae.

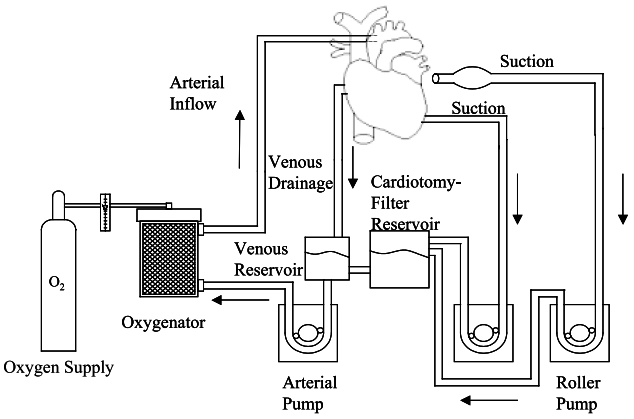

Fig. 11 Schematic of cardiovascular bypass circuit.

A significant complication associated with oxygenators in cardiopulmonary bypass is activation of the coagulation cascades and thrombosis. Patients are anticoagulated with heparin to achieve an activated clotting time (ACT) of 480 seconds to prevent thrombosis-related oxygenator failures.[37] Thrombus formation in the oxygenator can cause an increase in resistance to blood flow and a decrease in gas transfer. Thus, to reduce the risk of clot formation, oxygenators are designed to minimize regions of blood flow stasis, which typically promote thrombus formation. The high level of anticoagulation, however, can lead to an increased risk of bleeding.

Oxygenators and the entire bypass circuit are now being coated with heparin in order to prevent clotting in the circuit while reducing the required amount of systemic anticoagulation. There are several different heparin coatings currently available on the market.[38] The Carmeda Bioactive Surface has been used for more than a decade and utilizes a covalent end-point attachment of heparin to the surface. The BioLine Coating by Jostra first coats the surface with polypeptides and then with a low-molecular-weight heparin, Liquemin. The coating is available in two types, one for CBP and one for long-term use in extracorporeal membrane oxygenation. Other more recent coatings include AOThel by Artificial Organ Technology, Corline by Corline Systems AB, and the Trilium Biopassive Surface by Avecor. Many studies have been performed on the efficacy of the heparin coatings and the required level of systemic heparin with the coatings. Aldea et al.[39] compared noncoated circuits and an ACT of 480 seconds with coated circuits and an ACT of 280 seconds. The heparin coating resulted in a 34% decrease in the need for blood products, 13.8% less bleeding, 43.6% shorter intubation time, 41.7% less time in the intensive care unit, and 17.8% less time in the hospital compared with noncoated circuits.

Extracorporeal Membrane Oxygenation

Extracorporeal membrane oxygenation (ECMO) uses blood oxygenators in pump-driven external circuits to provide respiratory support and lung rest and recovery for prolonged periods of time (1–30 days).[40] ECMO is used in patients with severe lung failure who fail traditional mechanical ventilation. Similar to CPB circuits, the ECMO circuit contains a pump, a heat exchanger, and an oxygenator, but unlike CPB circuits, a venous reservoir and suctioning equipment is not used. In ECMO, the patient is continuously anticoagulated with heparin to achieve an ACT of 160–240 seconds, much less than that found in CPB.[41] The required blood flow in ECMO is 120 ml/kg/min for neonates, 75 ml/kg/min for pediatric, and 50 ml/kg/min for adults.[33] Extracorporeal membrane oxygenation is used to treat neonatal, pediatric, and adult patients with lung failure, and the effectiveness of ECMO differs in each of these groups. ECMO is most commonly used in neonates with a survival rate of 80%.[42] Indications for neonatal ECMO include meconium aspiration syndrome, respiratory distress syndrome, persistent fetal circulation, persistent pulmonary hypertension, and hyaline membrane disease.[43] Pediatric and adult patients have lower survival rates of 53% and 41%, respectively.[42] Indications for ECMO in pediatric or adult patients are viral, bacterial, or aspiration pneumonia and acute respiratory distress syndrome (ARDS), which can be caused by trauma, pneumonia, or sepsis.[44]

Three different cannulation techniques can be used in ECMO, including venovenous, venoarterial, and arteriovenous, referring to the locations of the blood drainage and return sites. Venovenous ECMO drains and returns to the venous system, venoarterial ECMO drains from the venous system and returns into the arterial system, and arteriovenous ECMO is the opposite. Venovenous (VV) ECMO was established in the 1960s and 1970s and is now the most commonly used cannulation technique.[33,45] VV ECMO has several different sites for cannulation including the internal jugular, saphenous, or femoral veins or the right atrium. In neonates, VV ECMO can use a single dual-lumen cannula or two cannulae. The single double-lumen cannula is used in the jugular vein, and the septum offset produces a larger channel for venous inflow into the ECMO circuit. The cannula must be designed to reduce recirculation of returned blood directly back into the ECMO circuit. Cardiac output, pump flow rate, cannula position, and right atrium size are all factors that can affect recirculation. Single double-lumen cannulation cannot be used in pediatric and adult ECMO due to inadequate venous inflow into the circuit and also high levels of hemolysis, recirculation, and pressure with flow rates greater than 600 ml/min.[45]

Venoarterial (VA) ECMO was the original cannulation technique used in ECMO and is indicated when cardiac support is required in addition to respiratory support. In contrast, VV ECMO provides no cardiac support and is not used in patients with cardiac arrest, arrhythmias, or myocardial failure.[45] The disadvantages of VA ECMO include cannulation of a major artery, lack of pulmonary perfusion, decreased cardiac output due to a higher afterload, and increased risk of neurological events. VV ECMO has several advantages over VA ECMO including preserving pulsatility and avoiding the cannulation of a major artery. Neurological events can also be reduced since thromboemboli from the circuit travel to the lungs instead of the brain. VV ECMO also prevents ischemic injury to the lungs since the lungs remain perfused with blood, but blood flow must be carefully regulated in order to prevent an imbalance in the central venous system.[45] Given its advantages compared to VA ECMO, several institutions are now using VV ECMO and comparing results with VA ECMO. Knight et al.[46] found an increased survival rate of 91% with VV ECMO compared to 80% with VA ECMO in neonates. Zahraa et al.[47] performed a retrospective study from 1986–1997 comparing VV and VA ECMO in pediatric patients and found a trend for improved survival with VV ECMO with survival rates of 60% and 56%, respectively.

The inflammatory and thrombogenic complications associated with cardiopulmonary bypass are exacerbated

in ECMO due to the longer blood exposure to the extracorporeal circuit. As for CPB circuits, ECMO circuits and oxygenators are heparin-coated to help minimize systemic heparinization, decrease inflammatory responses, and prevent thrombosis. One complication of ECMO not seen in CPB is plasma wetting of hollow fiber membranes from the longer-term exposure of the ECMO oxygenator to blood. Plasma wetting decreases gas exchange, can occur quickly and unpredictably, and requires replacement of the oxygenator. Microporous hollow fiber membranes can be coated with thin siloxane layers to prevent plasma wetting and increase the biocompatibility.[48–52] New polymer coatings are also being developed to resist plasma leakage while attenuating the inflammatory response. Saito et al.[52] coated CBP circuits with poly(2-methoxyethylacrylate) (PMEA) and compared the inflammatory response with that caused by uncoated circuits in swine. Protein adsorption was significantly less on the PMEA circuits compared with control (0.3 ± 0.03 $\mu g/cm^2$ versus 3.42 ± 0.04 $\mu g/cm^2$). Peek et al.[53] performed an initial clinical trial with the Medos Hilite 7000LT oxygenator, which uses a polymethyl pentene (PMP) asymmetric hollow fiber membrane, which was also coated with heparin. Additional studies are needed to fully evaluate the effectiveness of these new coated fiber oxygenators.

SUMMARY

Artificial lungs use bundles of microporous hollow fiber membranes made into modules designed to bring blood and gas phases in intimate contact separated by only the thin walls of the hollow fibers. This article reviewed the basic principles of gas exchange in hollow fiber-based artificial lungs. Artificial lungs used today are extracorporeal modules called blood oxygenators primarily employed for pulmonary support during open-heart surgical procedures involving cardiopulmonary bypass. To a much lesser degree, blood oxygenators are also used clinically to provide support to the failing lung in acute respiratory failure. Several research efforts are underway on the development of next-generation artificial lungs designed specifically for respiratory support of the failing lung either acutely or as a bridge to lung transplant in patients requiring chronic respiratory support. These efforts, reviewed in a companion article (see Lung, Artificial: Current Research and Future Directions), involve paracorporeal, intravascular, and intrathoracic devices. Approaches developed to specifically overcome limitations in gas exchange, biocompatibility, and other design factors of the present-day blood oxygenator are described in this article.

ACKNOWLEDGMENTS

Supported by HL70051 from the National Institutes of Health and by the U.S. Army Medical Research, Development, Acquisition, and Logistics Command under Grant No. DAMD17-98-1-8638. The views, opinions, and/or findings contained in this article are those of the authors and should not be construed as an official Department of the Army position, policy, or decision unless so designated by other documentation. KH is a recipient of a graduate fellowship in biomedical engineering from the Whitaker Foundation.

ARTICLES OF FURTHER INTEREST

Lung, Artificial: Current Research and Future Directions, p. 922
Lung Surfactants, p. 932

REFERENCES

1. http://www.lungusa.org/data. (accessed May 2001).
2. Demling, R.H. The modern version of adult respiratory distress syndrome. Annu. Rev. Med. **1995**, *46*, 193–202.
3. Zilberberg, M.D.; Epstein, S.K. Acute lung injury in the medical ICU: Co-morbid conditions, age, etiology, and hospital outcome. Am. J. Respir. Crit. Care Med. **1998**, *157* (4 Pt. 1), 1159–1164.
4. Bartlett, R.H.; Roloff, D.W.; Custer, J.R.; Younger, J.G.; Hirschl, R.B. Extracorporeal life support: The University of Michigan experience. JAMA **2000**, *283* (7), 904–908.
5. http://www.lungusa.org/data. (accessed March 2000).
6. http://www.lungusa.org/data. (accessed March 2001).
7. Mortensen, J.; Bezzant, T. Risk and hazard of mechanical ventilation: A collective review of published literature. Dis.-Mon. **1994**, *40* (11), 2193–2196.
8. Weinacker, A.B.; Vaszar, L.T. Acute respiratory distress syndrome: Physiology and new management strategies. Annu. Rev. Med. **2001**, *52*, 221–237.
9. AAMI Standards and Recommended Practices. Association for the Advancement of Medical Instrumentation. Volume 2.1 Biomedical Equipment, Part 1, Equipment Therapy and Surgery Cardiovascular implants and artificial organs: Blood gas exchangers. AAMI **1996**, *7199*, 633–648.
10. Newhouse, M.T. Tennis anyone? The lungs as a new court for systemic therapy. CMAJ **1999**, *161* (10), 1287–1288.
11. Weibel, E.R. *The Pathway for Oxygen: Structure and Function in the Mammalian Respiratory System*; Harvard University Press: Cambridge, 1984.
12. Federspiel, W.J.; Sawzik, P.J.; Borovetz, H.S.; Reeder, G.D.; Hattler, B.G. Temporary Support of the Lungs—The Artificial Lung. In *The Transplantation and Replacement*

of Thoracic Organs; Cooper, D.K.C., Miller, L.W., Patterson, G.A., Eds.; Kluwer Academic Publishers: Boston, 1996; 717–728.
13. High, K.M.; Snider, M.T.; Bashein, G. Principles of Oxygenator Function: Gas Exchange, Heat Transfer, and Blood-Artificial Surface Interaction. In *Cardiopulmonary Bypass Principles and Practice*; Gravlee, G.P., Davis, R.F., Utley, J.R., Eds.; Williams & Wilkins: Philadelphia, 1993; 28–54.
14. LaPierre, R.A., Jr.; Howe, R.J.; Haw, M.P.; Elliott, M. Oxygenators for Pediatric Cardiac Surgery. In *Cardiopulmonary Bypass in Neonates, Infants and Young Children*; Jonas, R.A., Elliott, M.J., Eds.; Butterworth-Heinemann: Boston, 1994; 173–185.
15. Beckley, P.D.; Holt, D.W.; Tallman, R.D., Jr. Oxygenators for Extracorporeal Circulation. In *Cardiopulmonary Bypass: Principles and Techniques of Extracorporeal Circulation*; Mora, C.T., Ed.; Springer-Verlag: New York, 1995; 199–219.
16. Lund, L. Measurement of Hollow Fiber Membrane Permeance in a Gas–Liquid System. Ph.D.; University of Pittsburgh, 2000.
17. Hattler, B.G.; Federspiel, W.J. Gas Exchange in the Venous System: Support for the Failing Lung. In *The Artificial Lung*; Vaslef, S.N., Anderson, R.W., Eds.; Landes Bioscience, 2002; 133–174.
18. Kamo, J.; Uchida, M.; Hirai, T.; Yosida, H.; Kamada, K.; Takemura, T. A new multilayered composite hollow fiber membrane for artificial lung. Artif. Organs **1990**, *14* (5), 369–372.
19. Montoya, J.P.; Shanley, C.J.; Merz, S.I.; Bartlett, R.H. Plasma leakage through microporous membranes. Role of phospholipids. ASAIO J. **1992**, *38* (3), M399–M405.
20. Mottaghy, K.; Oedekoven, B.; Starmans, H.; Muller, B.; Kashefi, A.; Hoffmann, B.; Bohm, S. Technical aspects of plasma leakage prevention in microporous capillary membrane oxygenators. ASAIO Trans. **1989**, *35* (3), 640–643.
21. Mulder, M. Preparation of Synthetic Membranes. In *Basic Principles of Membrane Technology*; Kluwer Academic Publishers: Boston, 1996; 71–156.
22. Niimi, Y.; Ueyama, K.; Yamaji, K.; Yamane, S.; Tayama, E.; Sueoka, A.; Kuwana, K.; Tahara, K.; Nose, Y. Effects of ultrathin silicone coating of porous membrane on gas transfer and hemolytic performance. Artif. Organs **1997**, *21* (10), 1082–1086.
23. Probstein, R.F. Solutions of Uncharged Molecules. In *Physicochemical Hydrodynamics*; John Wiley & Sons, Inc.: New York, 1994; 53–107.
24. Hewitt, T.J.; Hattler, B.G.; Federspiel, W.J. A mathematical model of gas exchange in an intravenous membrane oxygenator. Ann. Biomed. Eng. **1998**, *26* (1), 166–178.
25. Mockros, L.F.; Leonard, R.J. Compact cross-flow tubular oxygenators. ASAIO Trans. **1985**, *31*, 628–632.
26. Vaslef, S.N.; Cook, K.E.; Leonard, R.J.; Mockros, L.F.; Anderson, R.W. Design and evaluation of a new, low pressure loss, implantable artificial lung. ASAIO J. **1994**, *40* (3), M522–M526.
27. Vaslef, S.N.; Mockros, L.F.; Anderson, R.W.; Leonard, R.J. Use of a mathematical model to predict oxygen transfer rates in hollow fiber membrane oxygenators. ASAIO J. **1994**, *40* (4), 990–996.
28. Wickramasinghe, S.R.; Semmens, M.J.; Cussler, E.L. Mass transfer in various hollow fiber geometries. J. Membr. Sci. **1992**, *69*, 235–250.
29. Yang, M.C.; Cussler, E.L. Designing hollow fiber contactors. AIChE J. **1986**, *32*, 1910–1916.
30. Vaslef, S.N.; Mockros, L.F.; Cook, K.E.; Leonard, R.J.; Sung, J.C.; Anderson, R.W. Computer-assisted design of an implantable, intrathoracic artificial lung. Artif. Organs **1994**, *18* (11), 813–817.
31. Capatano, G.; Papenfuss, H.D.; Wodetzki, A.; Baurmeister, U. Mass and momentum transport in extra-luminal flow (ELF) membrane devices for blood oxygenation. J. Membr. Sci. **2001**, *184* (1), 123–135.
32. Dierickx, P.W.; De Wachter, D.S.; De Somer, F.; Van Nooten, G.; Verdonck, P.R. Mass transfer characteristics of artificial lungs. ASAIO J. **2001**, *47*, 628–633.
33. Hirschl, R. Devices. In *ECMO Extracorporeal Cardiopulmonary Support in Critical Care*; Zwischenberger, J.B., Bartlett, R.H., Eds.; Extracorporeal Life Support Organization: Ann Arbor, MI, 1995; 159–190.
34. http://www.americanheart.org/presenter.jhtml?identifier=4674. (accessed November 2002).
35. Bartlett, R.H. Physiology of Extracorporeal Life Support. In *ECMO Extracorporeal Cardiopulmonary Support in Critical Care*; Zwischenberger, J.B., Bartlett, R.H., Eds.; Extracorporeal Life Support Organization: Ann Arbor, MI, 1995; 27–52.
36. Galletti, P.M.; Colton, C.K. Artificial Lungs and Blood–Gas Exchange Devices. In *The Biomedical Engineering Handbook*; Bronzino, J.D., Ed.; CRC Press LLC: Boca Raton, 2000; 1–19.
37. Gravlee, G.P. Anticoagulation for Cardiopulmonary Bypass. In *Cardiopulmonary Bypass Principles and Practice*; Gravlee, G.P., Davis, R.F., Utley, J.R., Eds.; Williams & Wilkins: Philadelphia, 1993; 340–380.
38. Wendel, H.P.; Ziemer, G. Coating-techniques to improve the hemocompatibility of artificial devices used for extracorporeal circulation. Eur. J. Cardio-Thorac. Surg. **1999**, *16* (3), 342–350.
39. Aldea, G.S.; Doursounian, M.; O'Gara, P.; Treanor, P.; Shapira, O.M.; Lazar, H.L.; Shemin, R.J. Heparin-bonded circuits with a reduced anticoagulation protocol in primary CABG: A prospective, randomized study. Ann. Thorac. Surg. **1996**, *62*, 410–418.
40. Zwischenberger, J.B.; Bartlett, R.H. An Introduction to Extracorporeal Life Support. In *ECMO Extracorporeal Cardiopulmonary Support in Critical Care*; Zwischenberger, J.B., Bartlett, R.H., Eds.; Extracorporeal Life Support Organization: Ann Arbor, MI, 1995; 11–14.
41. Dark, J.H. Extracorporeal Respiratory Support. In *Techniques in Extracorporeal Circulation*; Kay, P.H., Ed.; Butterworth-Heinemann Ltd.: Boston, 1992; 309–320.
42. Tracy, T., Jr.; DeLosh, T.; Stolar, C. The Registry of the Extracorporeal Life Support Organization. In *ECMO Extracorporeal Cardiopulmonary Support in Critical Care*; Zwischenberger, J.B., Bartlett, R.H., Eds.; Extracorporeal

Life Support Organization: Ann Arbor, MI, 1995; 251–260.
43. Ichiba, S.; Bartlett, R.H. Current status of extracorporeal membrane oxygenation for severe respiratory failure. Artif. Organs **1996**, *20* (2), 120–123.
44. Mols, G.; Loop, T.; Geiger, K.; Farthmann, E.; Benzing, A. Extracorporeal membrane oxygenation: A ten-year experience. Am. J. Surg. **2000**, *180* (2), 144–154.
45. Cornish, J.; Clark, R. Principles and Practice of Venovenous Extracorporeal Membrane Oxygenation. In *ECMO Extracorporeal Cardiopulmonary Support in Critical Care*; Zwischenberger, J.B., Bartlett, R.H., Eds.; Extracorporeal Life Support Organization: Ann Arbor, MI, 1995; 87–110.
46. Knight, G.R.; Dudell, G.G.; Evans, M.L.; Grimm, P.S. A comparison of venovenous and venoarterial extracorporeal membrane oxygenation in the treatment of neonatal respiratory failure. Crit. Care Med. **1996**, *24* (10), 1678–1683.
47. Zahraa, J.N.; Moler, F.W.; Annich, G.M.; Maxvold, N.J.; Bartlett, R.H.; Custer, J.R. Venovenous versus venoarterial extracorporeal life support for pediatric respiratory failure: Are there differences in survival and acute complications? Crit. Care Med. **2000**, *28* (2), 521–525.
48. Shimono, T.; Shomura, Y.; Tahara, K.; Hioki, I.; Tenpaku, H.; Maze, Y.; Hirano, R.; Shimpo, H.; Shionoya, Y.; Yokoyama, A.; Morikan, T.; Yada, I. Experimental evaluation of a newly developed ultrathin silicone layer coated hollow fiber oxygenator. ASAIO J. **1996**, *42* (5), M451–M454.
49. Shimono, T.; Shomura, Y.; Hioki, I.; Shimamoto, A.; Tenpaku, H.; Maze, Y.; Onoda, K.; Takao, M.; Shimpo, H.; Yada, I. Silicone-coated polypropylene hollow-fiber oxygenator: Experimental evaluation and preliminary clinical use. Ann. Thorac. Surg. **1997**, *63* (6), 1730–1736.
50. Watanabe, H.; Hayashi, J.; Ohzeki, H.; Moro, H.; Sugawara, M.; Eguchi, S. Biocompatibility of a silicone-coated polypropylene hollow fiber oxygenator in an in vitro model. Ann. Thorac. Surg. **1999**, *67* (5), 1315–1319.
51. Shimamoto, A.; Kanemitsu, S.; Fujinaga, K.; Takao, M.; Onoda, K.; Shimono, T.; Tanaka, K.; Shimpo, H.; Yada, I. Biocompatibility of silicone-coated oxygenator in cardiopulmonary bypass. Ann. Thorac. Surg. **2000**, *69* (1), 115–120.
52. Saito, N.; Motoyama, S.; Sawamoto, J. Effects of new polymer-coated extracorporeal circuits on biocompatibility during cardiopulmonary bypass. Artif. Organs **2000**, *24* (7), 547–554.
53. Peek, G.J.; Killer, H.M.; Reeves, R.; Sosnowski, A.W.; Firmin, R.K. Early experience with a polymethyl pentene oxygenator for adult extracorporeal life support. ASAIO J. **2002**, *48* (5), 480–482.

Marcel Dekker, Inc.
270 Madison Avenue, New York, New York 10016